ISBN: 978-3-95450-214-1 ISSN: 2673-5490 doi:10.18429/JACoW-IPAC2021-WEPAB256

THREE-DIMENSIONAL SPACE CHARGE OSCILLATIONS IN A HYBRID PHOTOINJECTOR

M. Carillo*[1], F. Bosco[1], L. Giuliano[1], A. Mostacci[1], M. Migliorati[1], L. Palumbo[1], L. Ficcadenti
INFN-Sez.Roma1, Roma, Italy
L. Faillace[1], M. Behtouei, A. Giribono, B. Spataro, C. Vaccarezza
INFN-LNF, Frascati, Italy
J. Rosenzweig, UCLA, Los Angeles, California, USA
[1]also at La Sapienza University of Rome, Rome, Italy

Abstract

A new hybrid C-band photoinjector, consisting of a standing wave RF gun connected to a travelling wave structure, operating in a velocity bunching regime, has shown to produce an extremely high brightness beam with very low emittance and a very high peak current through a simultaneous compression of the beam in the longitudinal and transverse dimensions. A beam slice analysis has been performed in order to understand the evolution of the relevant physical parameters of the beam in the longitudinal and transverse phase spaces along the structure. A simple model for the envelope equation has been developed to describe the beam behavior in this particular dynamics regime that we term "triple waist", since all three dimensions reach a minimum condition almost simultaneously. The model explicitly analyzes the transverse envelope dynamics at the exit of the hybrid photoinjector, in the downstream drift where the triple waist occurs. The analytical solutions obtained from the envelope equation are compared with the simulations, showing a good agreement. Finally, these results have been analyzed also in terms of plasma oscillation to obtain a further physical interpretation of the beam dynamics.

INTRODUCTION

In the context of a collaboration between UCLA/Sapienza/INFN-LNF/RadiaBeam, a new hybrid C-band photo-injector [1–3] has been designed for the production of a very high brightness electron beam [4].
An electron beam generated by a standing wave (SW) RF gun is injected into a travelling wave (TW) accelerating section, at a zero-crossing phase voltage, where it experiences a longitudinal compression [5]. The system works in the velocity bunching regime which permits very high values of peak current and low values of normalized emittance. The triple waist occurs downstream the TW section in a drift section, where we are interested in studying the evolution of the physical parameters of the electron beam. The drift has a length of ~ 0.5 m after which one or more linac sections are installed.

OPTIMIZED BEAM DYNAMICS

The beam dynamics simulation were performed using the GPT code [6] with an initial bi-Gaussian distribution having a total charge of 250 pC, which obtains the results we describe here. In Fig. 1 we report the energy and the normalized emittance along the hybrid structure. In the RF gun the electron beam is accelerated up to an the energy of 4.42 MeV, which remains nearly constant in the drift tube (red curve Fig. 1). In the field-free region we note that emittance oscillates with a minimum value of 0.6 µmrad. In Fig. 2 we show the trend of rms bunch dimensions. The beam is focused by the external solenoid around the structure and reaches a waist at ~ 0.64 m from the cathode. The bunch length initially increases because of the space charge forces and as soon as it enters into the TW section, it begins to be compressed by a longitudinal focusing due to the RF voltage. The rms longitudinal size reaches a minimum of 400 fs at ~ 0.90 m from the cathode.

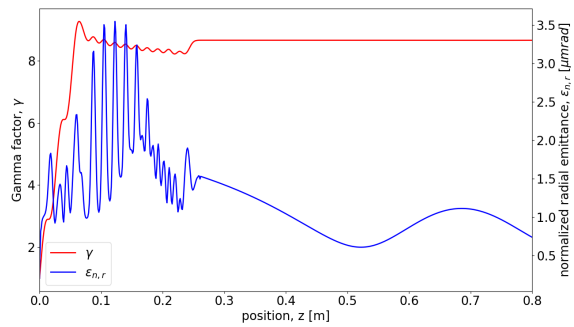

Figure 1: Optimized beam parameters: relativistic gamma factor (red line) and rms radial normalized emittance (blue line).

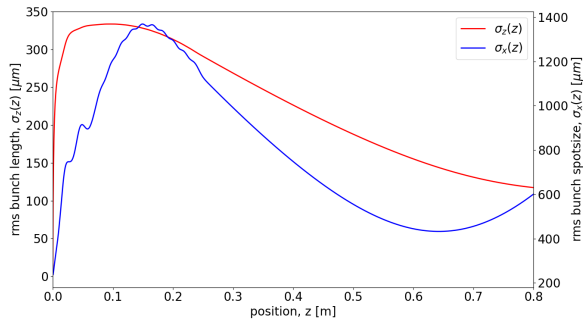

Figure 2: Rms bunch dimensions: rms length (blue line) and transverse spot size (red line).

* carillo.1596853@studenti.uniroma1.it

ISBN: 978-3-95450-214-1 ISSN: 2673-5490 doi:10.18429/JACoW-IPAC2021-WEPAB256

BEAM SLICE ANALYSIS

A more detailed analysis of the beam dynamics was performed by studying the evolution of individual slices of the beam. In fact, we split the bunch into 10 longitudinal slices at the cathode source and we observed their behavior along the structure. In Fig. 3 we show a) the initial slice partition, b) the transverse phase-space of the slices and c) the longitudinal phase space of the slices. We observe that there is a correlation of phase-space shapes, in both longitudinal and transverse planes, with the slice position. Then, the evolution of such slice distributions and phase-spaces were monitored during the bunch motion.

We observed the expected behavior due to velocity bunching [7], space charge effects, compression and the interpenetration of the slices. The results of these effects are apparent in Fig. 4 which shows an elliptical beam shape near the waist position and the modified transverse and longitudinal phase spaces. It's worth noting that, a significant correlation of the longitudinal phase space persists during the motion while slices tend to overlap in the transverse phase space.

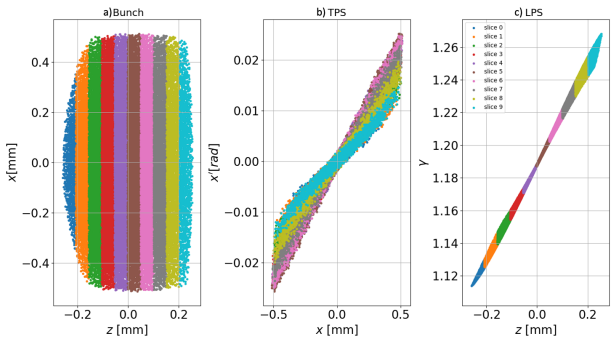

Figure 3: (a) Slices partition at the cathodes, (b) Slices transverse phase space, (c) Energy-position correlation.

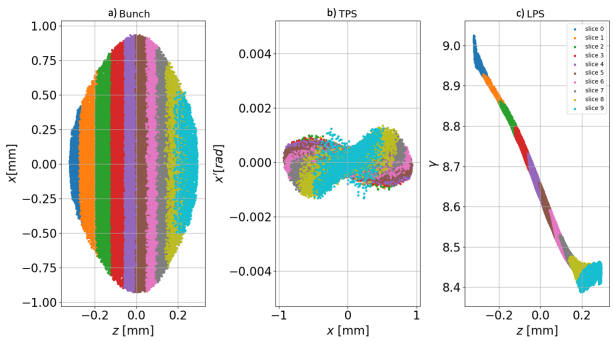

Figure 4: Modified bunch (a) shape and (b) transverse and (c) longitudinal phase space properties at the transverse waist ($z = 0.64$m).

ENVELOPE ANALYSIS IN THE DRIFT

In order to study the dynamics in the drift we recognize that the beam envelope equation is affected only by the space charge term, which dominates the effects of emittance pressure [8, 9]

$$\sigma_x'' = \frac{\kappa}{\sigma_x}, \tag{1}$$

where the derivation is with respect to z. The beam perveance κ depends on the current and therefore on the longitudinal distribution of charge: $\kappa = K/\sigma_z$ where now

$$K = \frac{N r_e f}{\sqrt{2\pi}\gamma^3}\frac{\sigma_{x,0}}{\sigma_{z,0}}, \tag{2}$$

and $\sigma_{x,0}$ and $\sigma_{z,0}$ are the rms dimensions at the waist. Here f is a geometric factor used for finite beams, which depends on the electric flux distribution on the bunch surface. For instance, if we consider the electric field in the three directions of an ellipsoidal distribution [10] similar to that observed near the waist in our present case, we obtain $f \sim 0.341$.

To derive an approximate simple model of the transverse beam evolution we start from the evidence of the simultaneous compression in the three dimensions which occurs in the drift (Fig 2), due to the external focusing of the solenoid (transverse plane) and to the energy chirp of the RF voltage (longitudinal plane). Accordingly, the envelope equation (Eq. ()1)) is solved using the approximation $\sigma_z \propto \sigma_x = \sigma$, that we call "triple waist" approximation:

$$\sigma'' = \frac{K}{\sigma^2}. \tag{3}$$

Exact Solution of the Envelope Equation

By integration we can derive the solution of Eq. (3):

$$z(\sigma) = z_0 + \frac{\sigma_0^{3/2}}{\sqrt{2K}}\Big[\ln\Big(\sqrt{\frac{\sigma}{\sigma_0}} + \sqrt{\frac{\sigma}{\sigma_0} - 1}\Big) + \sqrt{\frac{\sigma}{\sigma_0}\Big(\frac{\sigma}{\sigma_0} - 1\Big)}\Big]. \tag{4}$$

where the initial conditions are set at the waist z_0: $\sigma(z_0) = \sigma_0$ and $\sigma'(z_0) = \sigma_0' = 0$.

In Eq. (4), the position z is positive-definite and function of σ. In fact, it provides an implicit expression for σ, and we therefore make a comparison with the simulation data from GPT by plotting z as a function of σ_x (Fig. 5). The overlap of the two curves in Fig. 5 is rather good, especially in the vicinity of the waist.

Perturbative Solution of the Envelope Equation

In order to find an explicit solution for $\sigma(z)$ from Eq. (3), we apply a perturbative method often employed for nonlinear differential equations. We use the method in two steps, we first assume $\sigma = \sigma_0$, the value at waist for the RHS of Eq. (3)

$$\sigma'' = \frac{K}{\sigma_0^2} \tag{5}$$

whose integration yields

$$\sigma(z) = \sigma_0\Big[\frac{K}{2\sigma_0^3}z^2 + 1\Big]. \tag{6}$$

ISBN: 978-3-95450-214-1 ISSN: 2673-5490 doi:10.18429/JACoW-IPAC2021-WEPAB256

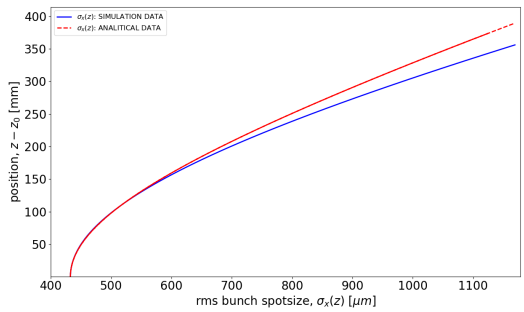

Figure 5: Longitudinal position along the machine as a function of the rms bunch spot size: comparison of z from equation 4 (red dashed line) with simulation data (blue line).

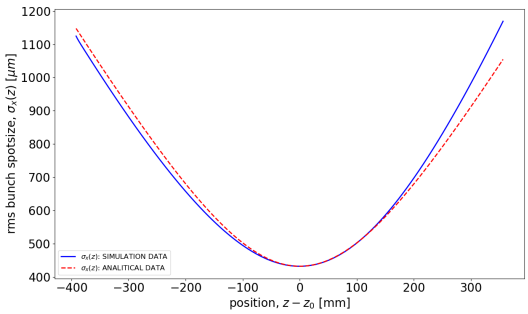

Figure 6: Rms bunch spot size as function of the longitudinal position along the machine: comparison perturbed solution (red dashed line) with simulation data (blue line).

Then, we substitute the above expression in the RHS of Eq. (3), and integrate, obtaining the following perturbative explicit solution of σ as function of z:

$$\sigma(z) = \sigma_0\Big[\sqrt{\frac{K}{2\sigma_0}}\Big(\frac{z}{\sigma_0}\Big)\tan^{-1}\Big(\sqrt{\frac{K}{2\sigma_0}}\Big(\frac{z}{\sigma_0}\Big)\Big)\Big]. \quad (7)$$

In Fig. 6 perturbative solution of Eq. (7) is compared with the GPT simulation data. Also in this case, a good agreement is observed between the two curves. The overlap is excellent near the waist position, and very good in the compression region $z < z_0$, while it loses precision as we move far downstream the waist.

CONNECTION TO FINITE-DIMENSION SINGLE-COMPONENT PLASMA OSCILLATIONS

For a further investigation of the beam dynamics, the envelope analysis has been related to the concept of plasma oscillations [8]. In charged particles distributions, the plasma frequency is often defined as the frequency of small density oscillations. One typically may write, in a beam with density n_b in equilibrium with the surrounding forces (ions, solenoid focusing), the small density oscillations in terms of a simple linearized equation:

$$\frac{d^2 n_b}{dt^2} + \omega_p^2 n_b = 0. \quad (8)$$

For a beam traveling with velocity v_b in the z direction, the plasma frequency is given by

$$\omega_b^2 = \frac{4\pi e^2 n_b}{\gamma_b^3 m_e}. \quad (9)$$

The plasma oscillation equation can be written the for the case of a particle beam by changing the independent variable to z:

$$\frac{d^2 n_b}{dz^2} + k_p^2 n_b = 0, \quad (10)$$

where $k_p = \frac{\omega_p}{v_b}$.

The beam density can be written as $n_b \simeq C/\sigma_x^3$ were C is a constant that depends on the number of particle. So taking the second derivative at the waist with respect to z, a relationship between the envelope equation and plasma oscillation is obtained:

$$\frac{d^2 n_b}{dz} = \frac{d^2}{dz^2}\left(\frac{C}{\sigma_x^3}\right) = -\frac{3n_b}{\sigma_x}\frac{d^2\sigma_x}{dz^2} = -\frac{3k}{\sigma_0}n_b = k_p^2 n_b, \quad (11)$$

where in the second step the condition $\sigma_x' = 0$ at the waist has been applied. Finally we have made a connection to the plasma frequency concept, even though there is no restoring force present, in the vicinity of the waist. This connection can be clarified in terms of a geometric factor f by comparing Eq. (3) with Eq. (11).

CONCLUSION AND FUTURE GOALS

The beam dynamics of a C-Band hybrid photo-injector has been studied in the downstream drift where the simultaneous longitudinal and transverse focusing occur. From the slice analysis, the properties and physical effects of the beam have been observed. In particular the evolution of the beam shape allowed us to use the correct distribution in analytical studies. The beam envelope equation in drift was analyzed and compared with simulations using the "triple waist" approximation. An excellent agreement was found especially in the neighborhood of the waist zone. Starting from this results, a more detailed analysis of the model describing the dynamics will be developed. We will solve the longitudinal equation in the drift so that a more accurate transverse equation can be obtained. A study concerning emittance compensation will be performed, starting from the results obtained with the slice analysis and with the analytical model we developed. The goal is to understand reduce the normalized emittance of the hybrid photo-injector, in order to achieve beams of higher brightness.

ACKNOWLEDGMENTS

This work is supported by DARPA GRIT under contract no. 20204571 and partially by INFN National committee V through the ARYA project.

ISBN: 978-3-95450-214-1 ISSN: 2673-5490 doi:10.18429/JACoW-IPAC2021-WEPAB256

REFERENCES

[1] L. Faillace *et al.*, "Beam Dynamics for a High Field C-Band Hybrid Photoinjector", presented at the 12th Int. Particle Accelerator Conf. (IPAC'21), Campinas, Brazil, May 2021, paper WEPAB051, this conference.

[2] B. Spataro *et al.*, "RF properties of a X-band hybrid photoinjector", *Nuclear Instruments and Methods in Physics Research Section A*, vol. 657, no. 1, pp. 99-106, 2011. doi:10.1016/j.nima.2011.04.057

[3] J. B. Rosenzweig *et al.*, "Design and applications of an X-band hybrid photoinjector", *Nuclear Instruments and Methods in Physics Research Section A*, vol. 657, pp. 107-113, 2011. doi:10.1016/j.nima.2011.05.046

[4] J. B. Rosenzweig *et al.*, "Next generation high brightness electron beams from ultrahigh field cryogenic rf photocathode sources", *Physical Review Accelerators and Beams*, vol. 22, no. 2, p. 023403, 2019. doi:10.1103/PhysRevAccelBeams.22.023403

[5] A. Fukasawa *et al.*, "Progress on the Hybrid Gun Project at UCLA", *Physics Procedia*, vol. 52, pp. 2-6, 2014. doi:10.1016/j.phpro.2014.06.002

[6] GPTSite, http://www.pulsar.nl/gpt/index.html

[7] D. Filippetto *et al.*, "Phase space analysis of velocity bunched beams", *Physical Review Special Topics - Accelerators and Beams*, vol. 14, p. 092804, 2011. doi:10.1103/PhysRevSTAB.14.092804

[8] J. B. Rosenzweig, *Fundamentals of Beam Physics*. New York, USA: Oxford University Press, 2003.

[9] M. Migliorati *et al.*, "Intrinsic normalized emittance growth in laser-driven electron accelerators", *Physical Review Special Topics - Accelerators and Beams*, vol. 16, p. 011302, 2013. doi:10.1103/PhysRevSTAB.16.011302

[10] O. Kellogg, *Foundation of Potential Theory*. Dover, UK: Springer, 1953.